Fracture mechanism of some brittle metallic glasses

J. X. Zhao,[1] R. T. Qu,[1] F. F. Wu,[1,2] Z. F. Zhang,[1,a)] B. L. Shen,[3] M. Stoica,[4] and J. Eckert[4,5]
[1]*Shenyang National Laboratory for Materials Science, Institute of Metal Research, Chinese Academy of Sciences, Shenyang 110016, People's Republic of China*
[2]*School of Materials and Chemical Engineering, Liaoning University of Technology, 169 Shiying Street, Jinzhou 121001, People's Republic of China*
[3]*Ningbo Institute of Materials Technology and Engineering, Chinese Academy of Sciences, Ningbo 315201, People's Republic of China*
[4]*Institute for Complex Materials, IFW Dresden, P.O. Box 270016, D-01171 Dresden, Germany*
[5]*Institute of Materials Science, TU Dresden, D-01062 Dresden, Germany*

(Received 24 December 2008; accepted 6 April 2009; published online 27 May 2009)

A systematic study on the fracture surface of brittle Mg-, Fe-, and Co-based metallic glasses under compressive loading is approached and a fracture mechanism is proposed. Experimentally, the metallic glass samples are compressed into many small fragments, displaying an explosion fracture feature. Therefore, an energy equilibrium model is employed to describe the fracture processes of those brittle metallic glasses. Furthermore, some regular nanoscale steps, which were scarcely discovered, are found on the mirror region on their fracture surfaces. It is suggested that such nanoscale steps are associated with the energy distribution in metallic glasses and are created by the shear waves generated by the instability of crack propagation during the explosion rupture processes. Based on the comparison of experimental observations with numerical calculations, we recommend a novel model for interpreting the development of nanoscale steps on the dynamic fracture surfaces of these brittle metallic glasses, which appropriately describes the experimental findings. © *2009 American Institute of Physics*. [DOI: 10.1063/1.3129313]

I. INTRODUCTION

Because of their superior mechanical properties, metallic glasses have triggered extensive scientific interest over the years.[1–4] Theoretically, metallic glasses can be considered as isotropic materials due to their disordered atomic arrangement.[5] With regard to experimental results, metallic glasses often fail along a narrow shear band under uniaxial tension and compression.[6–8] Recently, with the preparation of many new metallic glasses, some authors reported that metallic glassy samples often display a rather brittle fracture mode even under compression or bending loading conditions.[9–22] Moreover, many periodic nanoscale corrugations were found on the fracture surfaces of some Mg-, Fe-, Co-, and Ni-based metallic glasses which displayed obvious dynamic fracture features.[11–22] Such phenomena lead to many discussions about the dynamic fracture of metallic glasses and the formation mechanism of the nanoscale corrugations on the fracture surface. Thereby, Zhang *et al.*[13] investigated the cleavage fracture of Fe-based metallic glasses and considered the nanoscale steps on the fracture surface as the results of dynamic instability. Wang *et al.*[15] developed a model based on the meniscus instability and the plastic zone theory to describe the nanoscale periodic morphologies found on the fracture surface. Meng *et al.*[17] investigated the evolution of fracture upon dynamic loading of a tough metallic glass under high-velocity plate impact and proposed a model based on the fracture surface energy dissipation and void growth. The above investigations could explain the nanosteps from some perspectives; however, the intrinsic fracture mechanism of these metallic glasses has not been revealed clearly. Why do these metallic glasses compress into small pieces? What is the formation mechanism of the nanosteps[11–22] on the fracture surface? Why do these steps display different wavelengths[13] on the fracture surface? These questions lead to further researches about the fracture mechanism and the formation mechanism of the periodic steps on the dynamic fracture surfaces of these metallic glasses.

II. EXPERIMENTAL PROCEDURES

In this study, we carried out some compressive fracture tests on $Fe_{65.5}Cr_4Mo_4Ga_4P_{12}C_5B_{5.5}$, $Mg_{65}Cu_{7.5}Ni_{7.5}Zn_5Ag_5Y_{10}$, and $Co_{43}Fe_{20}Ta_{5.5}B_{31.5}$ metallic glass samples. First, Master ingots were prepared by arc-melting elemental powders with a purity of 99.9% or so. The master ingots were then remelted in a quartz tube using induction melting and injected into the copper mold in a purified inert atmosphere to obtain the rod samples with two dimensions, i.e., 2 mm in diameter and 30 mm in length. Then the casting alloys were cut into compressive specimens with dimensions of $\Phi 2.0 \times 4.0$ mm^2. Compression tests were conducted at a constant strain rate of 10^{-4} s^{-1} with an MTS 810 testing machine at room temperature. Unexpectedly, these specimens are compressed into many small fragments instead of the shear fracture. After fracture, the specimens were investigated by a LEO Supra 35 field emission high-resolution scanning electron microscope to reveal fracture features.

a)Author to whom correspondence should be addressed. Electronic mail: zhfzhang@imr.ac.cn.

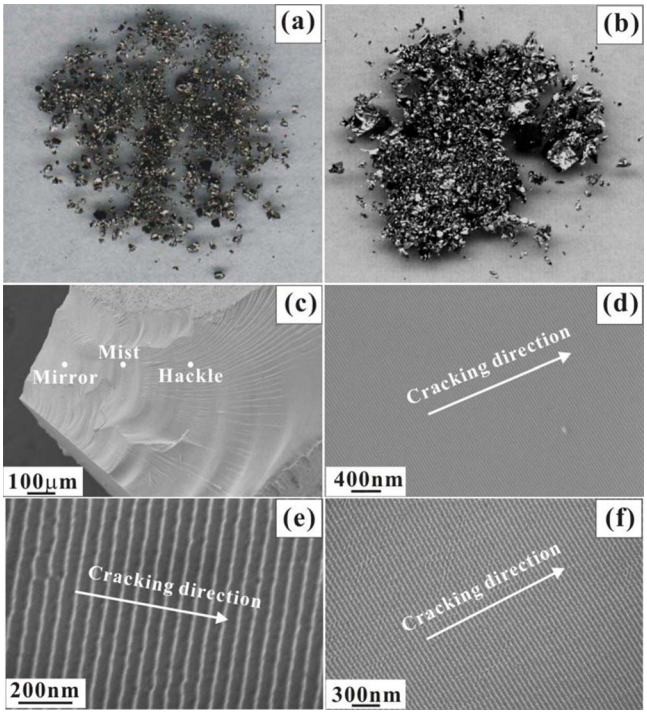

FIG. 1. (Color online) [(a) and (b)] The final photographs of $Co_{43}Fe_{20}Ta_{5.5}B_{31.5}$ and $Mg_{65}Cu_{7.5}Ni_{7.5}Zn_5Ag_5Y_{10}$ metallic glass specimens separately after compression. (c) Macroscopic brittle fracture surface of $Co_{43}Fe_{20}Ta_{5.5}B_{31.5}$ metallic glass under compression. [(d)–(f)] Nanoscale steps formed on the fracture surfaces of $Co_{43}Fe_{20}Ta_{5.5}B_{31.5}$, $Fe_{65.5}Cr_4Mo_4Ga_4P_{12}C_5B_{5.5}$, and $Mg_{65}Cu_{7.5}Ni_{7.5}Zn_5Ag_5Y_{10}$ metallic glasses, respectively. The arrows indicate the crack propagation direction.

III. EXPERIMENTAL RESULTS

Figures 1(a) and 1(b) display the photographs of $Co_{43}Fe_{20}Ta_{5.5}B_{31.5}$ and $Mg_{65}Cu_{7.5}Ni_{7.5}Zn_5Ag_5Y_{10}$ metallic glass specimens after compression, separately. Figure 1(c) shows a typical macroscopic fracture surface of $Co_{43}Fe_{20}Ta_{5.5}B_{31.5}$ metallic glass. Just as suggested by the model proposed by Johnson and Holloway,[23] the fracture surface can be divided into three regions: mirror, mist, and hackle regions, as marked in Fig. 1(c). In the mirror region, however, there are many regular nanoscale steps, as displayed in Fig. 1(d) at larger magnification, which is quite different from the traditional mirror region observed, for example, in brittle polymers such as polymethyl methacrylate (PMMA).[23] Similar steps were also found on the fracture surfaces of $Fe_{65.5}Cr_4Mo_4Ga_4P_{12}C_5B_{5.5}$ and $Mg_{65}Cu_{7.5}Ni_{7.5}Zn_5Ag_5Y_{10}$ metallic glasses under compression, as shown in Figs. 1(e) and 1(f). Careful observations on these periodic steps reveal that their wavelength changes from the sample edge toward the end of the mirror region. According to the experimental results,[13] the wavelength of the nanoscale steps as a function of the crack propagation distance varies, as shown in Fig. 2. Similar nanoscale steps were also discovered in the mirror region of the fracture surface.[11–22] The wavelength of the steps is typically in the range of 10–100 nm and appears to vary along the crack propagation direction.

IV. DISCUSSION

According to the above introduction, under the compressive loading, some Fe-, Mg-, and Co-based metallic glasses

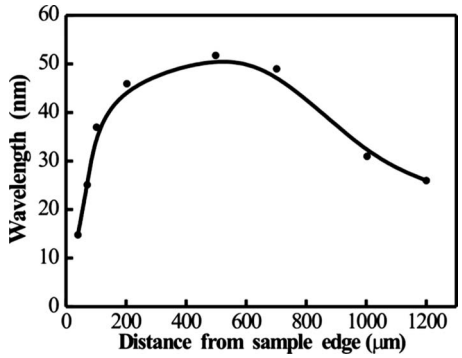

FIG. 2. Dependence of the wavelength of the nanoscale steps on the distance from the sample edge for $Fe_{65.5}Cr_4Mo_4Ga_4P_{12}C_5B_{5.5}$ metallic glass as taken from Ref. 13.

are separated into many small fragments when the compressive stress reaches the compressive strength. The fracture process is instantaneous and looks like an explosion process. In Ref. 24, the concept of explosion fracture was proposed to interpret the explosion phenomena. It was also pointed out that the high-strength metallic glasses and brittle materials might show explosion fracture under high external force.[24] Based on the experimental phenomena, one can conclude that the fracture of these metallic glasses belongs to the explosion fracture resulting from the dynamic fracture instabilities. For the explosion fracture, the crack propagation is a complicated event. In fact, with the crack expanding, huge energy in materials is forced to be released. At the same time, several kinds of shock waves could affect on the crack surface and bump up the crack velocity.[24] As a result, the materials could be broken into some fragments. Furthermore, owing to the intrinsic brittleness, metallic glass has often been investigated as conventional brittle materials.[13] Thereby, it is necessary to consider the fracture features in those brittle materials. For the mechanism of crack propagation, Fineberg *et al.*[25] investigated the instability of dynamic fracture in a brittle PMMA experimentally. It is found that the crack velocity increased shakily at the beginning and oscillated around a relatively stable value in the end. Remmers *et al.*[26] simulated the dynamic crack propagation in brittle solids and found a similar crack velocity behavior as Fineberg *et al.*[25]

In order to reveal the fracture mechanism in brittle metallic glasses, one can explain the fracture mode[25,26] in the brittle materials in a simple way. On the fracture process, the crack propagation could be thought to take place by the local tensile stress in spite of the compressive loading since the sample was separated into many small pieces in a very high velocity. For this consideration, based on the Griffith's brittle fracture theory,[27] neglecting the heat energy and the luminous energy during fracture, according to a crack system with constant-displacement loading,[28] one can take the following energy-balance formulation:

$$U_L = U_E + U_S + U_K. \quad (1)$$

Here, U_L is the energy of the external applied loading system (external work), where U_E is the elastic strain energy stored in the medium; U_S and U_K represent the fracture surface

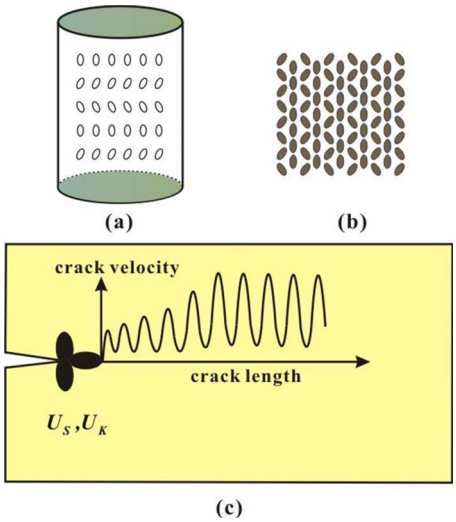

FIG. 3. (Color online) (a) Schematic of the explosion fracture in this experiment. (b) Illustration of the crack velocity variation in the fracture process.

energy and kinetic energy, respectively. Here, U_K is given by[28]

$$U_K = \pi E \varepsilon_A^2 c^2 \{1/[1+\alpha(c/c_0)^2]^2 - (c_0/c) \times (2-c_0/c)/(1+\alpha)^2\}, \quad (2)$$

wherein ε_A is the fixed strain during the course of fracture, c_0 and c represent the initial crack length and the crack length during propagation, respectively, and E stands for the elastic modulus. α is defined by the relation[28]

$$\alpha = 2\pi c_0^2/A, \quad (3)$$

in which A represents the plate area of the specimen.[28] Thus, the crack velocity v_c can be expressed as

$$v_c = (2\pi E/\kappa\rho)^{1/2}\{1-(c_0/c) \times (2-c_0/c) \times [(1+\alpha c^2/c_0^2)/(1+\alpha)]^2\}^{1/2}, \quad (4)$$

wherein $v_t=(2\pi E/\kappa\rho)^{1/2}$ is the terminal crack velocity with $v_c < v_t$, κ is a numerical constant,[28] and ρ is the medium density.

According to the hypothesis and numerical results,[28] during the fracture process of brittle materials, the curves of v_c and U_K pass through a maximum and then drop again in the process of the crack propagation. We can apply this theory to interpret the fracture mechanism of brittle metallic glasses in detail. At the beginning, owing to the brittleness and the external force, many microcracks appear in all spaces of the material body, as illustrated in Fig. 3(a). Then, the microcracks expand with an accelerated velocity. Meanwhile, the value of U_S increases according to $U_S=4c\gamma$,[28] in which γ expresses the unit area of fracture energy. In this situation, U_E, U_K, and U_S are enlarged in the earlier stage. According to Eq. (1), when the increment of U_L cannot satisfy the need of U_E, U_S, and U_K, ν_c and U_K will drop in order to accumulate the external work U_L. On account of the sustaining external force, U_L can increase to a high enough value to accelerate the crack velocity for another time, and U_S and U_K will increase again in another stage. After several stages, when the material could not support so many energies, it would be broken into small fragments along each performed crack surfaces, as shown in Fig. 3(b). Therefore, during the dynamic fracture process, these stages create accelerated and decelerated periods of the crack velocity and the crack rate can repeat several similar periods in order to accommodate the energy distribution, just as shown in Fig. 3(c). So, the crack velocity in fracture process displays a similar behavior as described in Refs. 25 and 26. In addition, we can also find some direct proofs from the experimental results. As shown in Fig. 1(c), the three regions (mirror, mist, and hackle) represent the fracture processes. In the mirror region, the surface is smooth which can be regarded as the initial stage of the crack propagation. In this stage, the crack velocity is in relatively low value. However, for the mist and hackle regions, the surfaces are in rough patterns and several vein structures are formed. It is concluded that the crack velocity in these regions is high enough, and the dynamic fracture instability appears. At the stages, many kinds of shock waves generated by strong kinetic energy effect on the crack surface and accelerate the crack propagation. When the material body cannot support the huge energy, the whole body is broken into many small fragments to release the energy, and the explosion fracture occurs.

Furthermore, some nanoscale steps were found in the mirror region of the fracture surface. In addition to the current results, recently, there are also some other reports on this aspect. For example, the nanoscale steps have been observed in different metallic glasses under various loading conditions, as summarized in Table I. Normally, the wavelength of the nanoscale steps is less than 100 nm and some scholars proposed some ideas to interpret the formation mechanism in some ways,[11–22] such as the fluid meniscus theory[14–16,18] and the energy dissipation theory.[17] However, those proposed mechanisms could not interpret the nanoscale steps thoroughly, the essence of the formation processes may not be successfully understood owing to the complex fracture processes. In this paper, we believed that such nanoscale steps were produced by the shear waves excited by the instabilities of crack propagation but not the results of local melting. If the local region is smelted, the crack velocity could be brought down. Unfortunately, the crack velocity is high continuously during the whole fracture process. Therefore, for interpreting the formation of the nanoscale steps, a novel model involving shear waves generated from the explosion fracture is applied to interpret the experimentally observed nanoscale steps on the fracture surface of brittle metallic glasses, which are perpendicular to the crack propagation direction (see Fig. 1). As illustrated in Fig. 4(a), it is hypothesized that the entire energy of the material is gathered in the crack system within the circular domain, and the shear wave is generated on the crack tip during the explosion fracture.[24] The shear wave energy U_{wave} can be regarded as one part of the kinetic energy. According to Eq. (2), we have

$$U_{\text{wave}} = \xi U_K = \xi \pi E \varepsilon_A^2 c^2 \{1/[1+\alpha(c/c_0)^2]^2 - (c_0/c) \times (2-c_0/c)/(1+\alpha)^2\}. \quad (5)$$

Here, the parameter ξ stands for the proportion of U_{wave} in

TABLE I. Simple summary of nanoscale steps on mirror region in different metallic glasses

Investigators	Compositions	Loading conditions	Wavelength (nm)
Shen *et al.*[a]	$Ni_{42}Cu_5Ti_{20}Zr_{21.5}Al_8Si_{3.5}$	Compression	~60
Xi *et al.*[b]	$Mg_{65}Cu_{25}Tb_{10}$	Three-point bending	~90
Zhang *et al.*[c]	$Fe_{65.5}Cr_4Mo_4Ga_4P_{12}C_5B_{5.5}$	Compression	0~70
Wang *et al.*[d]	$Fe_{73.5}Cu_1Nb_3Si1_{3.5}B_9$	Tension	30–60
Wang *et al.*[e]	$Mg_{65}Cu_{25}Tb_{10}$, etc.	Three-point bending	77–103
Wang *et al.*[f]	$Mg_{65}Cu_{25}Tb_{10}$	Bending	0–100
Meng *et al.*[g]	$Zr_{41.2}Ti_{13.8}Cu_{12.5}Ni_{10}Be_{22.5}$	High-velocity plate impact	~70
Wang *et al.*[h]	$Mg_{65}Cu_{25}Tb_{10}$	Tension, bending, etc.	32–56
Jiang *et al.*[i]	$Zr_{41.2}Ti_{13.8}Cu_{10}Ni_{12.5}Be_{22.5}$	Tension, compression, etc.	~80
Pan *et al.*[j]	$Mg_{65}Cu_{20}Ni_5Gd_{10}$, etc.	Three-point bending	~50
Li *et al.*[k]	$Fe_{78}Si_9B_{13}$	Tension	~100
Zhang *et al.*[l]	$Mg_{65}Cu_{25}Y_{10}$, etc.	Compression	~80

[a]Reference 11.
[b]Reference 12.
[c]Reference 13.
[d]Reference 14.
[e]Reference 15.
[f]Reference 16.
[g]Reference 17.
[h]Reference 18.
[i]Reference 19.
[j]Reference 20.
[k]Reference 21.
[l]Reference 22.

U_K. In the course of fracture, i.e., when providing more kinetic energy, U_{wave} accumulated ahead the crack tip is obviously enhanced. For simplification, one can suppose that the value of ξ is constant. Thus, the energy-flux density w can be expressed as[29]

$$w = \frac{U_{\text{wave}}}{t_0} = c_{s1}W, \tag{6}$$

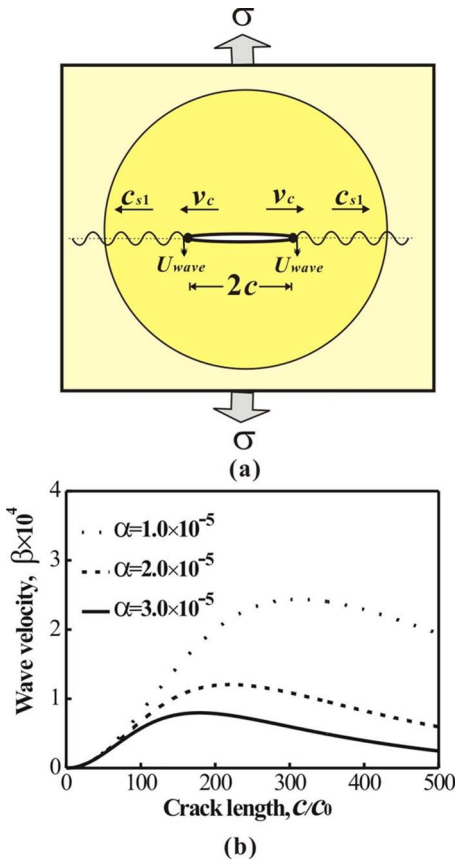

FIG. 4. (Color online) (a) Schematic of the crack system. (b) Dependence of the velocity of the shear wave c_{s1} on the increment of c/c_0 with different α.

$$c_{s1} = \frac{\xi U_K}{t_0 W} = \frac{\xi \pi E \varepsilon_A^2 c^2}{t_0 W}\{1/[1+\alpha(c/c_0)^2]^2 - (c_0/c) \times (2-c_0/c)/(1+\alpha)^2\} = \beta(c/c_0)^2\{1/[1+\alpha(c/c_0)^2]^2 - (c_0/c) \times (2-c_0/c)/(1+\alpha)^2\}. \tag{7}$$

Here, W stands for the whole energy comprised of a unit volume, c_{s1} is the wave velocity of the shear wave, t_0 is the propagation time for a shear wave, and $\beta = \xi \pi E \varepsilon_A^2 c_0^2 / t_0 W$. The semiquantitative relation for c_{s1} with increasing c/c_0 is shown in Fig. 4(b). For the unit time t_0, β is constant. With increasing c/c_0, the value c_{s1} first increases, goes through a maximum, and then decreases again. The shear wave ahead a crack tip can be considered as a transient wave that can be divided into many steady waves.[30] Therefore, one steady shear wave spreading in the isotropic medium can be expressed in a general form as[31]

$$u = A_0 e^{(ikx-\omega t)}. \tag{8}$$

In view of the extremely short time t in the fracture process, it is reasonable to rewrite Eq. (8) in a simplified form for quantitative analysis as

$$u = A_0 \sin(kx). \tag{9}$$

Here, u is the displacement perpendicular to the fracture surface, A_0 represents the amplitude of the shear waves, k stands for the wave number, $k = \omega / c_{s1}$, and ω and c_{s1} are the circular frequency and the velocity of the shear wave, respectively. In the current model, According to Eq. (7), it is considered that the wave velocity c_{s1} is a transient value because of the fracture instability. When the crack system is stable, the value c_{s1} can be regarded to approach the shear velocity c_s,[31] which is obtained in the steady-state system without cracks. Therefore, we have $c_{s1} \leq c_s$. For c_s, Wang *et al.*[15] pointed out that the velocity of the shear wave c_s in a metallic glass is about 2000 m/s, indicating that the value c_{s1} cannot exceed 2000 m/s. On the fracture surface, the distance between the

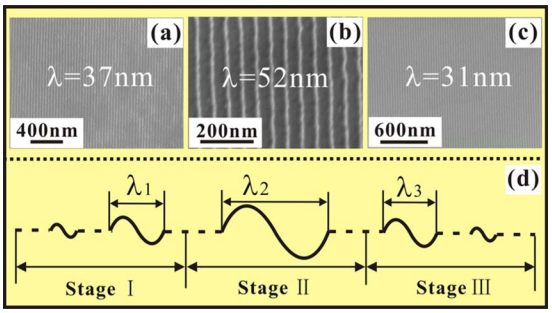

FIG. 5. (Color online) [(a)–(c)] Nanoscale steps with different wavelengths at different positions in the mirror region of the dynamic fracture surface for $Fe_{65.5}Cr_4Mo_4Ga_4P_{12}C_5B_{5.5}$ metallic glass. (d) Illustration of the formation of the nanoscale steps on the dynamic fracture surface. The dashed lines represent the different wave periods during the wavelength change event.

adjacent peaks of the periodic nanoscale steps can be approximately considered as the wavelength λ. Based on the relation $c_{s1}=f\lambda$,[30] in which the frequency f in the metallic glass is on the order of $\sim 10^4$ MHz,[12] the wavelength λ is less than ~200 nm, which agrees well with the previous experimental data, as listed in Table. I.[11–22] Hereby, many shear waves with different c_{s1} constitute the transient wave in the extending crack and result in the nanoscale steps on the fracture surface.

As displayed in Fig. 5, the whole fracture structures in the mirror region can be divided into three typical stages. First, the velocity of the shear waves increases simultaneously, considering the relation $c_{s1}=f\lambda$. Here, the frequency f is the essential parameter with a constant value. It is apparent that the value λ increases with the augment in c_{s1}; as a result, at stage I, c_{s1} and λ have relatively small values. The typical wavelength at this stage can be marked as λ_1, as shown in Fig. 5. When the crack expands sequentially, the energy distribution c_{s1} will reach its first peak. At this time, λ also becomes maximum, which corresponds to stage II where the kinetic energy reaches its first peak. The typical wavelength at stage II can be marked as λ_2. Afterward, c_{s1} drops in stage III. At this stage, the wavelength λ also exhibits a decreasing trend. In Fig. 5, λ_3 stands for the wavelength in this stage, which is smaller than λ_2. The three typical stages create the nanoscale steps with different wavelengths and the variation c_{s1} is illustrated in Fig. 5, and the tendency of the wavelength coincides with the results shown in Fig. 2.[13] It should be pointed out that the crack velocity in the mirror region is relatively small compared to that in the mist and hackle regions.[13] Hence, only low-energy shear waves contribute to the crack propagation. As a result, the fracture configuration in the mirror region displays rather smooth features macroscopically. However, when the crack extends, the huge mechanical energy increases the crack velocity. In this situation the crack tip will be susceptible to complicated wave structures and dynamic crack instabilities such as bifurcations[32] can appear on the fracture surface, as shown in Fig. 1(c). In the end, the material cannot accommodate even more energy and instantaneous fracture occurs.

V. CONCLUSIONS

On the basis of the fracture disciplines of brittle materials,[25,26] the fracture processes of those brittle metallic glasses can be ascribed to the energy distribution. In the process of crack propagation at very high velocity, the external work is transformed into elastic, kinetic, and surface energies. When the external work cannot supply the accretion of the elastic, kinetic, and surface energies, the crack velocity starts to drop. However, due to the external force, the external work can rapidly increase and push the crack velocity for another acceleration period. Therefore, for the brittle material, the crack velocity v_c in the course of crack extension becomes wavy, as in Fig. 3(c), and is similar to the previous results for other brittle materials.[25,26] At the same time, a shear wave exists during the explosion fracture, and the nanoscale steps on the dynamic fracture surface can be considered as an effect of the shear wave. The distance between two adjacent maxima of the nanoscale steps can be approximately regarded as the wavelength of the shear wave. Based on this principle, the calculated values of the wavelength λ are coincident with the experimental data.[13] Moreover, according to the observations,[13] the wavelength of the nanoscale steps on the fracture surfaces of metallic glasses have typical wavy appearance along the crack length, which is consistent with the variation in the wave velocity c_{s1}. In fact, the nanoscale steps were found only in the mirror region with a relatively low velocity.[13] When the crack velocity becomes high enough, the material breaks instantaneously and rough microstructures (mist and hackle regions) appear on the fracture surface.

ACKNOWLEDGMENTS

This work was financially supported by the National Natural Science Foundation of China (NSFC) under Grant Nos. 50625103, 50825103, and 50871117. One of the authors (Z.F.Z.) is also very grateful for the financial support of the Alexander-von-Humboldt (AvH) Foundation for a renewed research stay at IFW Dresden.

[1] H. S. Chen, Acta Metall. **22**, 1505 (1974).
[2] A. Inoue, Acta Mater. **48**, 279 (2000).
[3] Z. F. Zhang, F. F. Wu, G. He, and J. Eckert, J. Mater. Sci. Technol. **23**, 747 (2007).
[4] C. A. Schuh, T. C. Hufnagel, and U. Ramamurty, Acta Mater. **55**, 4067 (2007).
[5] W. H. Wang, C. Dong, and C. H. Shek, Mater. Sci. Eng. R **44**, 45 (2004).
[6] P. Lowhaphandu, S. L. Montgomery, and J. J. Lewandowski, Scr. Mater. **41**, 19 (1999).
[7] Z. F. Zhang, G. He, J. Eckert, and L. Schultz, Phys. Rev. Lett. **91**, 045505 (2003).
[8] C. T. Liu, L. Hwatherly, D. S. Easton, C. A. Carmichael, J. H. Schneibel, C. H. Chen, J. L. Wright, M. H. Yoo, J. A. Horton, and A. Inoue, Metall. Mater. Trans. A **29**, 1811 (1998).
[9] Y. K. Xu, H. Ma, J. Xu, and E. Ma, Acta Mater. **53**, 1857 (2005).
[10] Z. F. Zhang, H. Zhang, B. L. Shen, A. Inoue, and J. Eckert, Philos. Mag. Lett. **86**, 643 (2006).
[11] J. Shen, W. Z. Liang, and J. F. Sun, Appl. Phys. Lett. **89**, 121908 (2006).
[12] X. K. Xi, D. Q. Zhao, M. X. Pan, and W. H. Wang, Appl. Phys. Lett. **89**, 181911 (2006).
[13] Z. F. Zhang, F. F. Wu, W. Gao, J. Tan, Z. G. Wang, M. Stoica, J. Das, J. Eckert, B. L. Shen, and A. Inoue, Appl. Phys. Lett. **89**, 251917 (2006).
[14] G. Wang, Y. T. Wang, Y. H. Liu, M. X. Pan, D. Q. Zhao, and W. H. Wang, Appl. Phys. Lett. **89**, 121909 (2006).
[15] G. Wang, D. Q. Zhao, H. Y. Bai, M. X. Pan, A. L. Xia, B. S. Han, X. K. Xi, Y. Wu, and W. H. Wang, Phys. Rev. Lett. **98**, 235501 (2007).
[16] G. Wang, Y. N. Han, X. H. Xu, F. J. Ke, B. S. Han, and W. H. Wang, J. Appl. Phys. **103**, 093520 (2008).

[17]J. X. Meng, Z. Ling, M. Q. Jiang, H. S. Zhang, and L. H. Dai, Appl. Phys. Lett. **92**, 171909 (2008).
[18]G. Wang, K. C. Chan, X. H. Xu, and W. H. Wang, Acta Mater. **56**, 5845 (2008).
[19]M. Q. Jiang, Z. Ling, J. X. Meng, and L. H. Dai, Philos. Mag. **88**, 407 (2008).
[20]D. G. Pan, H. F. Zhang, A. M. Wang, Z. G. Wang, and Z. Q. Hu, J. Alloys Compd. **438**, 145 (2007).
[21]X. F. Li, K. F. Zhang, and G. F. Wang, J. Mater. Sci. Technol. **24**, 745 (2008).
[22]C. M. Zhang, X. Hui, Z. G. Li, and G. L. Chen, J. Alloys Compd. **467**, 241 (2009).
[23]J. W. Johnson and D. G. Holloway, Philos. Mag. **14**, 731 (1966).
[24]R. de Wit and W. C. Cooley, *Mechanics of Brittle Fracture* (McGraw-Hill, New York, 1979).
[25]J. Fineberg, S. P. Gross, M. Marder, and H. L. Swinney, Phys. Rev. Lett. **67**, 457 (1991).
[26]J. J. C. Remmers, R. de Borst, and A. Needleman, J. Mech. Phys. Solids **56**, 70 (2008).
[27]A. A. Griffith, Philos. Trans. R. Soc. London, Ser. A **221**, 163 (1921).
[28]B. Lawn, *Fracture of Brittle Solids* (Cambridge University Press, Cambridge, 1993).
[29]Z. P. Liao, *Introduction to Wave Motion Theories in Engineering* (Science, Beijing, 2002).
[30]Y. D. Feng, Y. S. Wang, and Z. M. Zhang, Acta Mech. solida. Sin. **23**, 3 (2002) (in Chinese).
[31]Z. L. Li and D. K. Liu, *Wave in Solid* (Science, Beijing, 1995).
[32]T. Cramer, A. Wanner, and P. Gumbsch, Phys. Rev. Lett. **85**, 788 (2000).